The Astrophysical Journal, 835:275 (10pp), 2017 February 1 doi:10.3847/1538-4357/835/2/275


# Flux and Polarization Variability of OJ 287 during the Early 2016 Outburst

Suvendu Rakshit[1], C. S. Stalin[1], S. Muneer[1], S. Neha[2,3], and Vaidehi S. Paliya[1,4]
[1] Indian Institute of Astrophysics, Block II, Koramangala, Bangalore-560034, India; suvenduat@gmail.com
[2] Aryabhatta Research Institute of Observational Sciences (ARIES), 263002, Nainital, India
[3] Pt. Ravishankar Shukla University, 492010, Raipur, India
[4] Department of Physics and Astronomy, Clemson University, Kinard Lab of Physics, Clemson, SC 29634-0978, USA
*Received 2016 August 4; revised 2016 December 21; accepted 2016 December 21; published 2017 February 1*

## Abstract

The gamma-ray blazar OJ 287 was in a high activity state during 2015 December–2016 February. Coinciding with this high brightness state, we observed this source for photometry on 40 nights in *R*-band and for polarimetry on nine epochs in *UBVRI* bands. During the period of our observations, the source brightness varied from 13.20 ± 0.04 mag to 14.98 ± 0.04 mag and the degree of polarization (*P*) fluctuated between 6.0% ± 0.3% and 28.3% ± 0.8% in *R*-band. Focusing on intranight optical variability (INOV), we find a duty cycle of about 71% using $\chi^2$-statistics, similar to that known for blazars. From INOV data, the shortest variability timescale is estimated to be 142 ± 38 minutes, yielding a lower limit of the observed Doppler factor $\delta_0 = 1.17$, the magnetic field strength $B \leqslant 3.8$ G, and the size of the emitting region $R_s < 2.28 \times 10^{14}$ cm. On internight timescales, a significant anticorrelation between *R*-band flux and *P* is found. The observed *P* at *U*-band is generally larger than that observed at longer-wavelength bands, suggesting a wavelength-dependent polarization. Using *V*-band photometric and polarimetric data from Steward Observatory obtained during our monitoring period, we find a varied correlation between *P* and *V*-band brightness. While an anticorrelation is sometimes seen between *P* and *V*-band magnitude, no correlation is seen at other times, thereby suggesting the presence of more than one short-lived shock component in the jet of OJ 287.

*Key words:* BL Lacertae objects: individual (OJ 287) – galaxies: photometry – polarization

*Supporting material:* data behind figure, figure set, machine-readable table

## 1. Introduction

OJ 287 is a well-known BL Lac object that shows a featureless continuum spectrum. It has been extensively studied for optical flux variability (Blake 1970; Andrew et al. 1971; O'Dell et al. 1978). The long-term optical light curve shows a well-defined 11.65 yr of periodicity between large outbursts (Sillanpaa et al. 1988). Several models have been proposed to explain the periodicity in outbursts, such as the binary black hole model with the primary having an accretion disk (Sillanpaa et al. 1988, 1996), quasi-periodic oscillations in an accretion disk (Igumenshchev & Abramowicz 1999), and a binary black hole without relativistic precession (Katz 1997; Villata et al. 1998; Valtaoja et al. 2000). Among them, a precessing binary black hole in which the secondary black hole affects the accretion disk of the primary is more favorable than others, as it predicts more accurately the timing of the major outburst (Sundelius et al. 1997; Valtonen & Ciprini 2012). OJ 287 has also been studied for polarization variability (Shakhovskoi & Efimov 1977; Sillanpaa et al. 1991, 1992; Pursimo et al. 2000; Valtaoja et al. 2000; Efimov et al. 2002; Villforth et al. 2009). Sillanpaa et al. (1991), based on the observations carried out over six nights, found anticorrelation between flux and polarization variations, which they explained as a result of highly rotating plasma inside a relativistic jet. However, Villforth et al. (2009) did not find any clear correlation between flux and polarization. From long-term (year-timescale) photopolarimetric observations, Efimov et al. (2002) noticed rapid continuous rotation of the position angle (PA) of about $4.^{\circ}92$ day$^{-1}$ in the clockwise direction, suggesting a helical magnetic field jet structure. OJ 287 is also known to show variability and flares at GeV $\gamma$-ray energy (Ciprini et al. 2009; Agudo et al. 2011; Escande & Schinzel 2011; Neronov & Vovk 2011).

OJ 287 was predicted to have a major outburst in 2015 by Valtonen et al. (2011). In line with the prediction, many episodes of flaring behavior have been noted since 2015 December. Shappee et al. (2015) and Valtonen et al. (2016) reported a strong optical flare on 2015 December 05, wherein they found an increase in brightness of about 1.5 mag. The WEBT/GASP project (Larionov et al. 2015) reported that the source reached maximum brightness in the *J*-band on 2015 December 04. During the same period, enhanced brightness was also reported by the SMARTS monitoring program (MacPherson et al. 2015) and also independently by Valtonen et al. (2015). In the X-ray band too, *Swift*/XRT observations (Ciprini et al. 2015; Wierzcholska & Siejkowski 2015; Valtonen et al. 2016) found the source in a high brightness level on 2015 December 05. The source was again detected in a flaring activity on 2016 February 05 (Zola et al. 2016).

We have been monitoring OJ 287 repeatedly for photometric and polarimetric variations since 2016 January (Muneer et al. 2016; Paliya et al. 2016). Here, we present our new *R*-band photometric observations obtained during 40 nights from 2016 January 07 to 2016 April 11, including 21 nights of intranight optical variability (INOV) and *UBVRI* polarimetry, including the ones already reported by us in Paliya et al. (2016) and Muneer et al. (2016), and *R*-band intranight polarization variability (INPV) on three nights. The main motivation behind this monitoring is to understand (i) the INOV nature of the source in its recent flaring state and (ii) the relation between total flux and polarization characteristics of the source. The paper is organized as follows. In Section 2 we present our observations and analysis; the results of our monitoring are

**Table 1**
Log of Photometric Observation

| Date (yyyy mm dd) (1) | $N$ (2) | Exp. Time (s) (3) | Duration (hr) (4) |
|---|---|---|---|
| 2016 Jan 07 | 2 | 300 | 0.2 |
| 2016 Jan 08 | 3 | 900 | 0.9 |

**Note.** Columns: (1) date of observations; (2) number of data points in DLC; (3) exposure time in seconds; (4) duration of monitoring in hours.

(This table is available in its entirety in machine-readable form.)

reported in Section 3, followed by a discussion in Section 4. We summarize our results in Section 5. We adopt a cosmology $H_0 = 70\,\mathrm{km\,s^{-1}\,Mpc^{-1}}$ and $q_0 = 0$.

## 2. Observation and Data Reduction

### 2.1. Photometry

Photometric observations in *R*-band were carried out with a 1k × 1k CCD attached to the 0.75 m telescope at the Vainu Bappu Observatory (VBO) in Kavalur, India. The CCD has a pixel size of 24 $\mu$m, image scale of $0\farcs48$ pixel$^{-1}$, gain of 1.01 e$^-$ ADU$^{-1}$, and readout noise of 11.51 e$^-$. Due to weather constraints, on some nights we were able to get only a few points, but on 21 nights we obtained more than 20 frames, which allowed us to study the INOV of the source. The source was suitably placed in the CCD so as to get at least three comparison stars given in Fiorucci & Tosti (1996). The log of the photometric observations is given in Table 1. The images were analyzed using standard procedures in IRAF.[5] To get the optimum aperture for aperture photometry, we followed the procedure described in Stalin et al. (2004).

### 2.2. Polarimetry

Polarimetric observations were carried out on a total of nine nights; of these, on six nights single-epoch multiband *UBVRI* observations were performed, and on three nights continuous monitoring was done in *R*-band. For polarimetric observations, two telescopes were used: the 104 cm telescope, located at VBO, and the 104 cm Sampurnand telescope, located at the Aryabhatta Research Institute for Observational Sciences (ARIES), Nainital. At the telescope at VBO, a three-band, double-beam photopolarimeter was used, the details of which can be found in Srinivasulu et al. (2015). We used a diaphragm of $20''$ diameter for the observations. In addition to the *UBVRI* bands, we also obtained polarimetric measurements in the light integrated in the $V - I$ spectral region; we refer to this band as $R'$. At ARIES, the ARIES Imaging Polarimeter (AIMPOL; Medhi et al. 2007) was used. A detailed description of AIMPOL and the techniques of polarization measurements may be found in Ramaprakash et al. (1998), Rautela et al. (2004), and Neha et al. (2016). All polarimetric data are presented in Table 2.

[5] IRAF is operated by the Association of Universities for Research in Astronomy, Inc., under cooperative agreement with the National Science Foundation.

**Table 2**
Results of Polarization Observations

| Date (yyyy mm dd) (1) | Band (2) | JD (3) | $P$ (%) (4) | $P_{\mathrm{error}}$ (%) (5) | PA (deg.) (6) | $\mathrm{PA_{error}}$ (deg.) (7) |
|---|---|---|---|---|---|---|
| 2016 Feb 12 | *U* | 2,457,431.3201 | 16.3 | 1.1 | 110.9 | 1.9 |
| 2016 Feb 12 | *B* | 2,457,431.3201 | 18.8 | 0.8 | 118.0 | 1.2 |
| 2016 Feb 12 | *V* | 2,457,431.3648 | 19.8 | 1.0 | 119.0 | 1.4 |
| 2016 Feb 12 | *R* | 2,457,431.3372 | 19.2 | 0.5 | 115.8 | 0.8 |
| 2016 Feb 12 | *I* | 2,457,431.3104 | 16.6 | 0.3 | 118.0 | 1.0 |
| 2016 Feb 12 | $R'$ | 2,457,431.2796 | 18.9 | 0.3 | 116.9 | 0.5 |
| 2016 Mar 08 | *U* | 2,457,456.2399 | 33.0 | 1.8 | 62.4 | 1.7 |
| 2016 Mar 08 | *B* | 2,457,456.2399 | 28.6 | 1.5 | 59.9 | 1.6 |
| 2016 Mar 08 | $R'$ | 2,457,456.1932 | 22.6 | 0.2 | 60.8 | 0.3 |
| 2016 Mar 09 | $R'$ | 2,457,457.1786 | 27.7 | 0.5 | 61.2 | 0.5 |
| 2016 Mar 10 | *U* | 2,457,458.2526 | 38.7 | 1.4 | 74.3 | 1.1 |
| 2016 Mar 10 | *B* | 2,457,458.2526 | 32.1 | 1.1 | 64.9 | 1.1 |
| 2016 Mar 10 | *V* | 2,457,458.2475 | 27.8 | 0.8 | 71.0 | 0.9 |
| 2016 Mar 10 | *R* | 2,457,458.2230 | 28.3 | 0.8 | 72.5 | 0.8 |
| 2016 Mar 10 | *I* | 2,457,458.2870 | 22.5 | 0.9 | 67.3 | 1.2 |
| 2016 Mar 10 | $R'$ | 2,457,458.2012 | 27.4 | 0.4 | 71.6 | 0.4 |
| 2016 Mar 11 | *U* | 2,457,459.2242 | 32.2 | 3.0 | 63.2 | 3.1 |
| 2016 Mar 11 | *B* | 2,457,459.2242 | 27.2 | 1.6 | 58.6 | 1.8 |
| 2016 Mar 11 | *V* | 2,457,459.2232 | 30.0 | 0.9 | 63.5 | 0.9 |
| 2016 Mar 11 | *R* | 2,457,459.1924 | 23.7 | 0.6 | 60.6 | 0.8 |
| 2016 Mar 11 | $R'$ | 2,457,459.1703 | 26.7 | 0.4 | 61.1 | 0.5 |
| 2016 Apr 04 | *U* | 2,457,483.1590 | 24.2 | 1.9 | 114.3 | 2.3 |
| 2016 Apr 04 | *B* | 2,457,483.1590 | 15.6 | 1.1 | 126.5 | 2.1 |
| 2016 Apr 04 | *V* | 2,457,483.1690 | 12.7 | 0.7 | 123.9 | 1.7 |
| 2016 Apr 04 | *R* | 2,457,483.1331 | 15.7 | 0.7 | 130.6 | 1.3 |
| 2016 Apr 04 | *I* | 2,457,483.2047 | 12.3 | 0.7 | 121.5 | 1.7 |
| 2016 Apr 04 | $R'$ | 2,457,483.1112 | 16.8 | 0.4 | 127.5 | 0.6 |
| 2016 Apr 05 | *R* | 2,457,484.1184 | 17.0 | 0.8 | 107.5 | 1.4 |
| 2016 Apr 05 | *R* | 2,457,484.1451 | 15.1 | 0.8 | 108.7 | 1.5 |
| 2016 Apr 05 | *R* | 2,457,484.1666 | 11.6 | 0.6 | 99.1 | 1.6 |
| 2016 Apr 05 | *R* | 2,457,484.1821 | 10.1 | 0.6 | 115.6 | 1.8 |
| 2016 Apr 05 | *R* | 2,457,484.1994 | 12.9 | 0.7 | 105.5 | 1.6 |
| 2016 Apr 05 | *R* | 2,457,484.2221 | 16.6 | 0.8 | 119.9 | 1.4 |
| 2016 Apr 06 | *R* | 2,457,485.1145 | 7.6 | 0.3 | 112.9 | 1.3 |
| 2016 Apr 06 | *R* | 2,457,485.1320 | 6.5 | 0.4 | 113.4 | 1.7 |
| 2016 Apr 06 | *R* | 2,457,485.1491 | 6.5 | 0.4 | 115.5 | 1.9 |
| 2016 Apr 06 | *R* | 2,457,485.1666 | 7.3 | 0.4 | 116.1 | 1.5 |
| 2016 Apr 06 | *R* | 2,457,485.1841 | 6.1 | 0.5 | 119.3 | 2.5 |
| 2016 Apr 06 | *R* | 2,457,485.2012 | 6.9 | 0.5 | 114.4 | 2.0 |
| 2016 Apr 06 | *R* | 2,457,485.2187 | 6.2 | 0.3 | 113.6 | 1.6 |
| 2016 Apr 06 | *R* | 2,457,485.2362 | 6.0 | 0.3 | 113.3 | 1.7 |
| 2016 Apr 10 | *R* | 2,457,489.1125 | 14.1 | 0.6 | 87.7 | 1.3 |
| 2016 Apr 10 | *R* | 2,457,489.1398 | 12.5 | 0.6 | 89.8 | 1.4 |
| 2016 Apr 10 | *R* | 2,457,489.1634 | 12.7 | 0.6 | 92.4 | 1.3 |
| 2016 Apr 10 | *R* | 2,457,489.1869 | 14.2 | 0.7 | 89.9 | 1.5 |
| 2016 Apr 10 | *R* | 2,457,489.2115 | 16.2 | 0.9 | 90.3 | 1.6 |

**Note.** Columns: (1) date of observation; (2) observing band ($R'$ is the integrated polarization in the *VRI* spectral region); (3) time in Julian day; (4) degree of polarization in percent; (5) error in degree of polarization in percent; (6) polarization position angle in degrees; (7) error in position angle in degrees.

## 3. Results

### 3.1. Intranight Optical Variability

To study INOV, we restricted ourselves to only observations carried out for a minimum of about 2 hr so as to ensure the availability of a sufficient number of photometric points to characterize INOV. Differential light curves (DLCs) of the OJ 287 were generated relative to two comparison stars present on

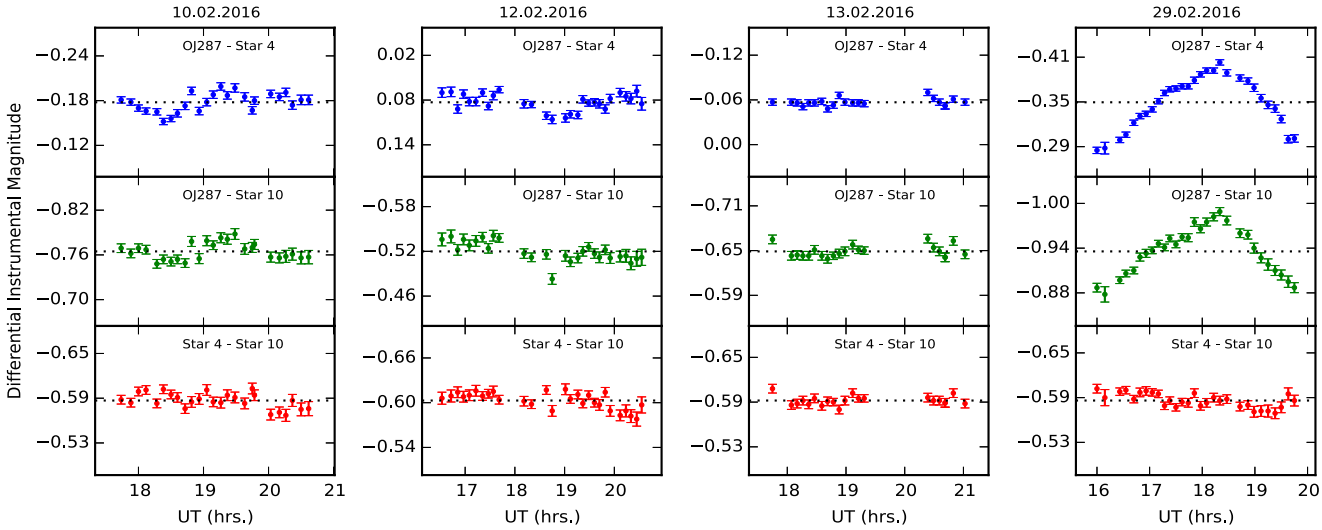


**Figure 1.** Intranight DLCs for OJ 287. From top to bottom the DLCs are for OJ 287–star 4, OJ 287–star 10, and star 4–star 10. The dates of observations are written on the top of each panel. The dotted black lines indicate the mean of the DLC. Stars 4 and 10 are those given by Fiorucci & Tosti (1996). Only four intranight DLCs are shown here, and the other 17 DLCs are available in the Figure Set.

(The complete figure set (21 images) is available.)

the same CCD frame as described in Section 2. We note that the chosen optimum aperture for photometry on each night is often close to the median FWHM and the host galaxy has negligible effects in our photometry (Cellone et al. 2000). Some DLCs are shown in Figure 1. In the star–star DLCs (with the comparison stars having similar brightness to OJ 287) at certain epochs, deviant points are noticed owing to nonphotometric sky conditions. Such data points are identified if they are greater than $2\sigma$, where $\sigma$ is the standard deviation of the star–star DLCs. The number of such deviant points that are removed amounts to the maximum of two data points each in less than half a dozen of the observing nights. To ascertain the variability nature of OJ 207 on any given night, we have employed three criteria, outlined below.

One method is based on the parameter $C$ given by Jang & Miller (1997). It is defined as the ratio of the standard deviation of the source and comparison star DLC ($\sigma_s$) and the comparison stars DLC ($\sigma$) and is given as $C = \sigma_s/\sigma$. As the DLCs of OJ 287 were generated relative to two comparison stars, we obtained two values of $C$. The source is considered variable only when both the values of $C \geqslant 2.576$ (see Paliya et al. 2013).

As an alternative to the widely used $C$-statistics, de Diego (2010) proposed the $F$-statistics. It is defined as the ratio of the variance of source and comparison star DLC ($\sigma_s^2$) and the comparison stars DLC ($\sigma^2$) and is given by $F = \sigma_s^2/\sigma^2$. To find the variability on any given night using the $F$ value, we compared both $F$ values (relative to the two comparison stars) with the critical $F$ value, $F_\nu^\alpha$, where $\alpha$ is the significance level and $\nu$ is the degrees of freedom ($\nu = N_p - 1$, where $N_p$ is the number of data points in the DLC). Following Paliya et al. (2013), we used $\alpha = 0.01$, which corresponds to a probability $p \geqslant 99\%$. The source is considered to be variable only if both the $F$ values are greater than $F_\nu^\alpha$.

We also used $\chi^2$-statistics (Kesteven et al. 1976) to characterize INOV. According to this, if the $\chi^2$ value of a DLC exceeds the critical value, $\chi^2_{\alpha,\nu}$, with significance $\alpha = 0.01$, then the source is considered variable. $\chi^2$-statistics is defined by

$$\chi^2 = \sum_{i=1}^{n} \frac{(D_i - \langle D \rangle)^2}{\epsilon_i^2}. \quad (1)$$

Here $\epsilon_i$ is the error of the measurement $D_i$, and $\langle D \rangle$ is defined as

$$\langle D \rangle = \frac{\sum_{i=1}^{n} \epsilon_i^{-2} D_i}{\sum_{i=1}^{n} \epsilon_i^{-2}}. \quad (2)$$

We calculated the amplitude of variability ($\Psi$; Romero et al. 1999) from the DLCs as $\Psi = 100\sqrt{(D_{\max} - D_{\min})^2 - 2\sigma^2}\,\%$. Here $D_{\max}$ and $D_{\min}$ are the maximum and the minimum, respectively, in the DLC of OJ 287 relative to the comparison stars, and $\sigma^2$ is the variance of the star–star DLC. Thus, corresponding to the two DLCs of the source with respect to the two comparison stars, we have two values of $\Psi$ on each night. The results of the $C$, $F$, and $\chi^2$-statistics and $\Psi$ for all 21 DLCs are given in Table 3.

We also estimated the duty cycle (DC) of INOV of OJ 287 using the definition of Romero et al. (1999),

$$\mathrm{DC} = 100 \frac{\sum_{i=1}^{n} N_i (1/\Delta t_i)}{\sum_{i=1}^{n} (1/\Delta t_i)}\ \%, \quad (3)$$

where $\Delta t_i = \Delta t_{i,\mathrm{obs}}(1+z)^{-1}$ is the duration of the monitoring session of the source on the $i$th night after cosmological redshift ($z$) correction. If INOV is detected, then $N_i = 1$; otherwise, $N_i = 0$. We find an INOV DC = 30% when variability was characterized using $C$-statistics. However, using $F$-statistics, the DC increased to 45%, and it further increased to 71% considering $\chi^2$-statistics. This enhanced DC is similar to what is known for blazars (Stalin et al. 2004).

We calculated the minimum variability timescale in our INOV data as $\tau = dt/\ln(F_1/F_2)$ following the definition given by Burbidge et al. (1974). Here, $dt$ is the time difference between any two flux measurements $F_1$ and $F_2$. From our observed DLCs we calculated all possible time differences $\tau_{ij}$

**Table 3**
Intranight Variability Properties

| Date (yyyy mm dd) (1) | Ψ1 (% ) (2) | Ψ2 (%) (3) | $F_1$ (4) | $F_2$ (5) | Status (6) | $C_1$ (7) | $C_2$ (8) | Status (9) | $\chi^2$ (10) | $\chi^2_{\alpha=0.01,\nu}$ (11) | Status (12) | $dt$ (hr) (13) |
|---|---|---|---|---|---|---|---|---|---|---|---|---|
| 2016 Feb 10 | 4.70 | 4.00 | 1.380 | 1.171 | NV | 1.175 | 1.082 | NV | 163.208 | 42.980 | V | 2.2 |
| 2016 Feb 12 | 4.00 | 5.80 | 1.026 | 1.365 | NV | 1.013 | 1.168 | NV | 122.299 | 46.963 | V | 3.1 |
| 2016 Feb 13 | 2.20 | 2.70 | 0.598 | 1.626 | NV | 0.773 | 1.275 | NV | 26.847 | 37.566 | NV | 2.5 |
| 2016 Feb 29 | 11.80 | 11.10 | 12.912 | 10.753 | V | 3.593 | 3.279 | V | 1932.985 | 48.278 | V | 2.9 |
| 2016 Mar 03 | 4.70 | 2.10 | 1.325 | 0.308 | NV | 1.151 | 0.555 | NV | 281.167 | 38.932 | V | 2.2 |
| 2016 Mar 06 | 9.00 | 10.30 | 17.322 | 14.964 | V | 4.162 | 3.868 | V | 1020.255 | 37.566 | V | 2.2 |
| 2016 Mar 07 | 4.90 | 5.50 | 6.707 | 9.300 | V | 2.590 | 3.050 | V | 284.627 | 34.805 | V | 1.8 |
| 2016 Mar 08 | 7.20 | 7.20 | 42.775 | 43.884 | V | 6.540 | 6.625 | V | 490.736 | 41.638 | V | 2.0 |
| 2016 Mar 09 | 4.80 | 4.80 | 9.294 | 7.986 | V | 3.049 | 2.826 | V | 218.527 | 37.566 | V | 1.8 |
| 2016 Mar 10 | 3.50 | 4.10 | 2.440 | 3.003 | NV | 1.562 | 1.733 | NV | 99.288 | 34.805 | V | 2.3 |
| 2016 Mar 11 | 3.70 | 3.90 | 3.916 | 4.508 | V | 1.979 | 2.123 | NV | 132.167 | 46.963 | V | 2.8 |
| 2016 Mar 27 | 3.89 | 2.38 | 1.310 | 0.471 | NV | 1.145 | 0.686 | NV | 29.150 | 38.932 | NV | 2.1 |
| 2016 Mar 29 | 3.30 | 3.00 | 4.958 | 4.507 | V | 2.227 | 2.123 | NV | 57.634 | 36.191 | V | 1.8 |
| 2016 Mar 30 | 2.70 | 3.60 | 0.747 | 1.174 | NV | 0.864 | 1.084 | NV | 47.865 | 45.642 | V | 2.5 |
| 2016 Mar 31 | 2.00 | 2.70 | 1.420 | 2.111 | NV | 1.192 | 1.453 | NV | 27.399 | 40.289 | NV | 2.3 |
| 2016 Apr 03 | 2.20 | 2.90 | 1.476 | 2.342 | NV | 1.215 | 1.530 | NV | 23.993 | 38.932 | NV | 2.0 |
| 2016 Apr 04 | 2.40 | 2.40 | 1.027 | 1.262 | NV | 1.013 | 1.123 | NV | 24.070 | 36.191 | NV | 2.0 |
| 2016 Apr 05 | 3.00 | 3.20 | 0.987 | 1.305 | NV | 0.993 | 1.142 | NV | 37.446 | 42.980 | NV | 2.2 |
| 2016 Apr 06 | 4.20 | 5.80 | 1.200 | 2.071 | NV | 1.095 | 1.439 | NV | 69.109 | 42.980 | V | 2.1 |
| 2016 Apr 07 | 10.10 | 10.40 | 14.908 | 13.025 | V | 3.861 | 3.609 | V | 484.825 | 42.980 | V | 2.2 |
| 2016 Apr 10 | 4.50 | 4.70 | 4.238 | 6.485 | V | 2.059 | 2.547 | NV | 110.030 | 40.289 | V | 2.0 |

**Note.** Columns: (1) date of observation; (2 and 3) INOV amplitudes in percent; (4 and 5) $F$ values computed for the OJ 287 DLCs relative to the steadiest pair of comparison stars (star 4 and star 10) on any night; (6) variability status according to $F$-statistics; (7 and 8) values of $C$ for the two OJ 287 DLCs relative to the two comparison stars (star 4 and star 10); (9) variability status as per $C$-statistics; (10) $\chi^2$ value; (11) critical value $\chi^2_{\alpha=0.01,\nu}$; (12) variability status as per $\chi^2$-statistics; (13) time duration of observation in hours.

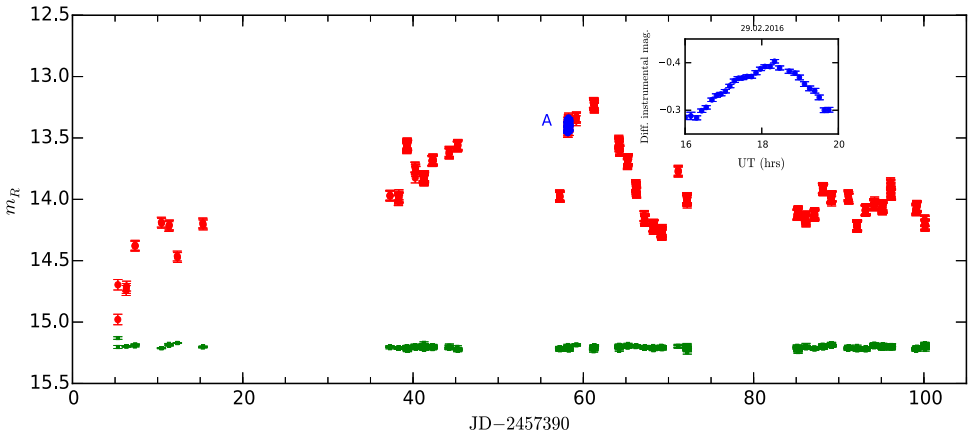


**Figure 2.** Long-term variation of $R$-band magnitude. The bunches of points in the plots are due to the intranight monitoring; one such bunch, denoted by "A," includes the DLC of 2016 February 29, shown in the inset. The DLC of star 4 and star 10 is shown at the bottom (square) after shifting by 15.8 mag. The data used to create this figure are available.

for all allowable pairs of observations for which $|F_i - F_j| > \sigma_{F_i} + \sigma_{F_j}$. From the ensemble of $\tau_{ij}$ values, the minimum timescale is obtained as $\tau_{\rm var} = \min[\tau_{i,j}]$. Here, $i$ runs from 1 to $n-1$, and $j$ runs from $i+1$ to $n$, where $n$ is the total number of data points. The uncertainties in the $\tau_{i,j}$ values are determined by propagating the errors in the flux measurements (Bevington 1969). Using this method on all the DLCs where INOV is detected, we find a minimum $\tau_{\rm var}$ of $142 \pm 38$ minutes in the observations done on 2016 April 07.

### 3.2. Long-term Optical Variability (LTOV)

The time span of our monitoring program is large enough to search for LTOV. The LTOV light curve of OJ 287 from 2016 January 07 to April 11 is shown in Figure 2. The magnitude of OJ 278 was calibrated using the three standard stars as mentioned in Section 3.1. Figure 2 shows that OJ 287 is variable on day-like timescales. During our monitoring program, a change of about 2 mag was found within a few days.

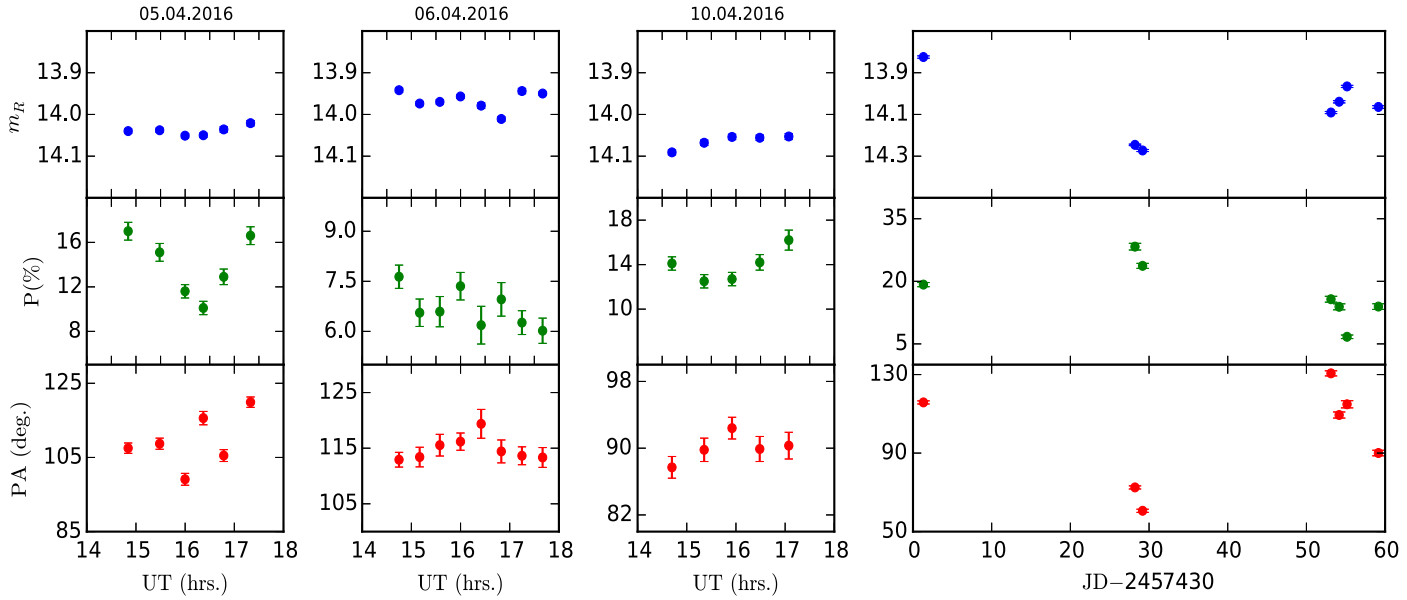


**Figure 3.** INPV of OJ 287. Shown from top to bottom are the variation of *R*-band magnitude ($m_R$), the degree of polarization (%), and PA (deg) as a function of UT (hr). The dates are shown in the top of each panel. The LTPV of OJ 287 is shown in the rightmost panel.

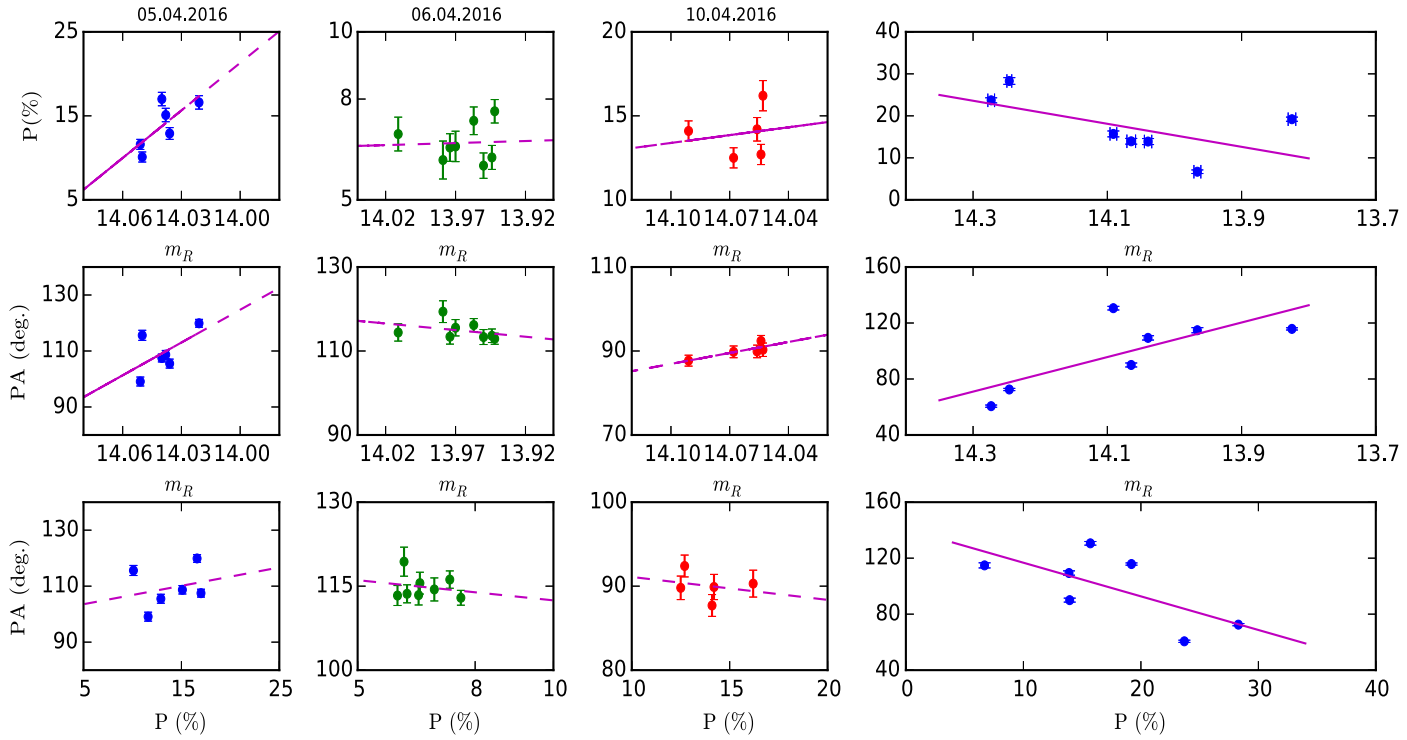


**Figure 4.** Plots *P* vs. $m_R$, PA vs. $m_R$, and PA vs. *P* for INPV. The dates are indicated on the top of each panel. The rightmost panel shows the correlation between different physical quantities based on LTPV observations. The lines are the linear least-squares fits to the data.

### *3.3. Polarization Variability*

INPV of OJ 287 has been studied earlier by Villforth et al. (2009), who found about 16% polarization. On the nights of 2016 April 05, 06, and 10, we have sufficient data points in *R*-band to characterize the INPV of OJ 287. The polarization properties displayed by the source on those three nights are plotted in the first three panels of Figure 3. We also have in total seven epochs of *R*-band polarization measurements between 2016 February and April. These observations are shown in the last panel of Figure 3. When more than one measurement is available on any particular night, we have taken their average value to study long-term polarization variability (LTPV). From this figure, it is clear that the source has shown both INPV and LTPV.

We also studied the correlation between different observed quantities, and the results are shown in Figure 4. The solid lines in these panels are the linear least-squares fits to the data. A correlation between brightness and *P* is found on 2016 April

**Table 4**
Results on the Correlation Analysis between Photometric and Polarimetric Observations

| Date (1) | Parameter (2) | $r_p$ (3) | Significance (4) |
|---|---|---|---|
| All | *F*–*P* | −0.66 | 0.000 |
| | *F*–PA | +0.75 | 0.000 |
| | *P*–PA | −0.62 | 0.001 |
| 2016 Apr 05 | *F*–*P* | +0.73 | 0.093 |
| | *F*–PA | +0.57 | 0.230 |
| | *P*–PA | +0.24 | 0.635 |
| 2016 Apr 06 | *F*–*P* | +0.04 | 0.909 |
| | *F*–PA | −0.33 | 0.416 |
| | *P*–PA | −0.19 | 0.646 |
| 2016 Apr 10 | *F*–*P* | +0.16 | 0.787 |
| | *F*–PA | +0.83 | 0.079 |
| | *P*–PA | −0.24 | 0.694 |

**Note.** Columns: (1) date of observation; (2) correlation between data sets; (3) Pearson correlation coefficient ($r_p$); (4) $p$ value for no correlation.

05. Less INPV was observed on 2016 April 06, with $P$ changing by only 1.5%, while PA changed by about 7°. On 2016 April 10, the source becomes fainter by about 0.2 mag than its brightness on 2016 April 06; however, $P$ increased by 7% and PA decreased by about 20°.

On the LTPV, we find a clear anticorrelation between source brightness and $P$. However, PA is found to be correlated with brightness. We also find a negative correlation between PA and $P$. Similar results have been found by Sillanpaa et al. (1991). The statistics of the correlation analysis between the photometric and polarimetric properties of OJ 287 are shown in Table 4.

To characterize INPV in our data, we used the $\chi^2$-statistics (see Section 3.1). We considered the source as variable in polarization if the $\chi^2$ value exceeds the critical value $\chi^2_{\alpha,\nu}$ with significance $\alpha = 0.01$. The fractional variability (FV) index of the source is defined by

$$\mathrm{FV} = \frac{A_{\max} - A_{\min}}{A_{\max} + A_{\min}}. \quad (4)$$

Here $A_{\max}$ and $A_{\min}$ are the maximum and minimum amplitudes, respectively, of variations in both $P$ and PA. The results of INPV are given in Table 5. The DC of INPV is found to be 81%, which is similar to the DC of about 77% found by Andruchow et al. (2005) for radio-selected BL Lacs, the category to which OJ 287 belongs.

Figure 5 shows the long-term variation of PA observed in the month of 2016 April. A linear least-squares fit to the data gives a rotation rate of $5\overset{\circ}{.}8\ \mathrm{day}^{-1}$. This rate is close to the rate of $4\overset{\circ}{.}92\ \mathrm{day}^{-1}$ found by Efimov et al. (2002). The observed $Q$ and $U$ parameters are plotted in Figure 5. The average values of $Q$ and $U$ are $\langle Q\rangle = -12.2 \pm 0.2\%$ and $\langle U\rangle = -0.1 \pm 0.2\%$, respectively. This deviates from the origin, implying the presence of a stable polarized component (see Jones et al. 1985).

### 3.4. Wavelength-dependent Polarization (WDP)

On a few epochs, we have polarization observations in *UBVRI* bands. The multiband polarization variations are shown in Figure 6. During all the epochs except that on 2016 February 12, $P$ in $U$-band is larger than the other bands, and thus OJ 287 showed WDP. The variation of $P$ as a function of wavelength for different nights is shown in Figure 6. From the figure, it is clear that on some epochs both $P$ and PA decrease with wavelength, although the anticorrelation of $P$ and wavelength is stronger than that of PA and wavelength.

## 4. Discussion

OJ 287 has shown remarkable optical flux and polarization variations during its recent bright state in 2015 December–2016 April. We find the source to show a large amplitude and a high duty cycle of INOV. A large-amplitude flare (0.12 mag) with a slow rise and fast declining pattern was found on 2016 February 29. Though the exact mechanisms for the cause of INOV are not known, the observations reported here can be used to put constraints on the physical characteristics of the source. From our INOV observations, we find the shortest timescale of variability, $\tau_{\mathrm{var}}$, of $142 \pm 38$ minutes on 2016 April 07 that sets an upper limit on the size of the emission region, $R_s < 19.5 \times 10^{14}\ (\delta/10)$ cm, where $\delta$ is the Doppler factor.

We estimated the observed Doppler factor, $\delta_o$, based on the relativistic beaming model (Marscher & Scott 1980; Aharonian et al. 2007; Xiang & Dai 2007). Following Bessell (1979), the observed monochromatic flux ($f_R$) is calculated from the apparent $R$-band magnitude ($m_R$) of OJ 287 (see Figure 2) as $f_R = 3.08 \times 10^{-23} 10^{-0.4 m_R}\ \mathrm{W\ m^{-2}\ Hz^{-1}}$. The observed source-frame monochromatic luminosity ($L_{\nu_s}$) at the frequency $\nu_s$ (considering $\nu_s$ as the $V$-band frequency) is calculated from $f_R$ using

$$L_{\nu_V} = 4\pi D_L f_R \left[\frac{\lambda_R}{\lambda_V (1+z)}\right]^{\alpha} (1+z)^{-1}, \quad (5)$$

where the luminosity distance $D_L = (cz/H_0)^2(1 + z/2)^2$, $\lambda_R$ and $\lambda_V$ are the effective central wavelengths of $R$ and $V$-band, respectively, and $\alpha$ is the spectral index. We used $\alpha = 1.62$, which is the average spectral index found by Efimov et al. (2002). Though blazars show spectral variations, the value of $\alpha$ used here is similar to the value found for OJ 287 and other blazars from power-law fits to broadband optical data (Williamson et al. 2014).

Following Elvis et al. (1994), we estimated the observed bolometric luminosity as $L_B = 13.2 \nu_V L_{\nu_V}$, where $\nu_V$ is the $V$-band frequency. Considering the fact that any strong outburst having energy $\Delta L = |L_i - L_j|$ must occur on a timescale larger than $t_{\min} = \tau_{\mathrm{var}}/(1+z) \ll t_{\mathrm{cross}}$ (light-crossing time of $R_s$), the inferred efficiency of accretion, $\eta_o$, can be calculated as $\eta_o \geqslant 5 \times 10^{-43}\ \Delta L/t_{\min}$ (Fabian & Rees et al. 1979, pp. 381–398). For our observed $\tau_{\mathrm{var}} = 142$ minutes, we find $t_{\min} = 108$ minutes, during which the bolometric luminosity has changed by $\Delta L = 4.33 \times 10^{45}\ \mathrm{erg\ s^{-1}}$, corresponding to $\eta_o = 0.33$. In the case of disk accretion, a rapidly rotating black hole has an intrinsic value of accretion efficiency ($\eta_i$) less than about 0.3 (Frank et al. 1986). As our calculated value is greater than 0.1, the observed INOV is due to relativistic beaming.

**Table 5**
Intranight Polarization Properties

| Date (yyyy mm dd) | $\langle P\rangle$ (%) | $\sigma_P$ | FV | $\chi^2_P$ | Status | $\langle$PA$\rangle$ (°) | $\sigma_{\rm PA}$ | FV | $\chi^2_{\rm PA}$ | Status |
|---|---|---|---|---|---|---|---|---|---|---|
| (1) | (2) | (3) | (4) | (5) | (6) | (7) | (8) | (9) | (10) | (11) |
| 2016 Apr 05 | 13.24 | 2.552 | 0.255 | 80.230 | V | 109.57 | 6.759 | 0.095 | 117.480 | V |
| 2016 Apr 06 | 6.73 | 0.539 | 0.119 | 15.701 | NV | 114.39 | 2.015 | 0.028 | 7.478 | NV |
| 2016 Apr 10 | 13.62 | 1.328 | 0.129 | 15.380 | V | 90.01 | 1.496 | 0.026 | 6.598 | NV |

**Note.** Columns: (1) date of observation; (2 and 3) mean and standard deviation of degree of polarization; (4) fractional polarization variability; (5) $\chi^2$ of $P$; (6) variable (V)/nonvariable (NV); (7–11) same as columns (2)–(6), but for position angle.

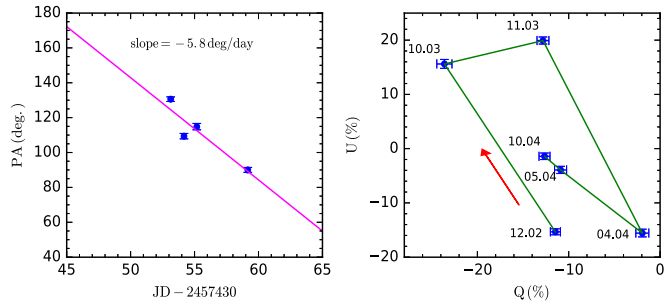


**Figure 5.** Left: rotation rate of polarization PA. A straight line has been fit to the 2016 April polarization data. The estimated slope is $-5.^{\circ}8$ day$^{-1}$. Right: plot of the equatorial Stokes $Q$ and $U$ parameters in the $Q$–$U$ plane in $R$-band. The arrow indicates the direction of rotation of the plane of polarization. The labels indicate the date of observations.

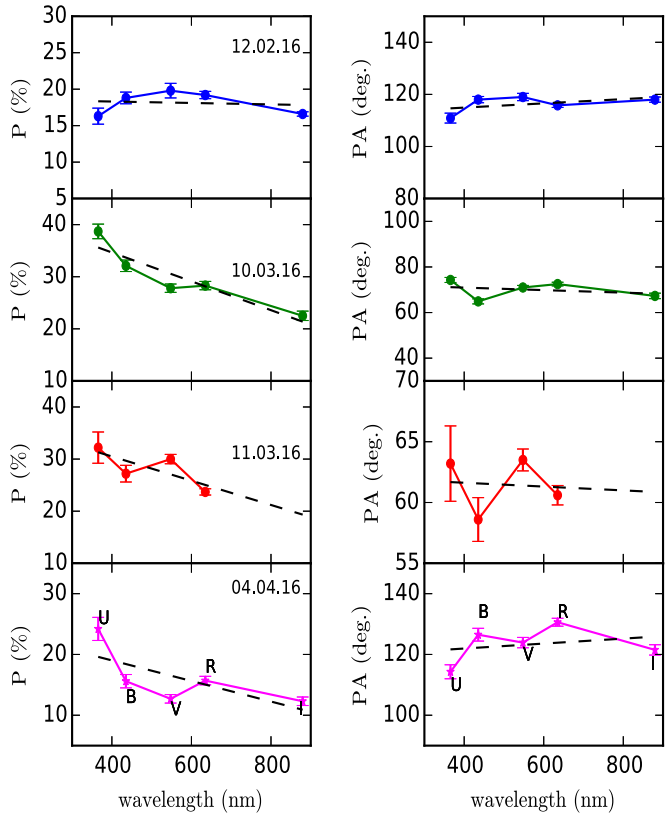


**Figure 6.** WDP. Degree of polarization (left panel) and polarization PA (right panel) are plotted as a function of wavelength for different dates of observations. The dashed line shows the linear fit to the data. Filter names are marked in the lower panels.

The $\delta_o$ can be computed from the relationships of $\Delta L(o) = \delta^{3+\alpha}\Delta L(i)$ and $t_{\rm min}(o) = \delta^{-1}t_{\rm min}(i)$ (Frank et al. 1986; Zhang et al. 2002), and using $\eta_o \geqslant 5 \times 10^{-43}\frac{\Delta L(o)}{t_{\rm min}(o)}$ and $\eta_i \geqslant 5 \times 10^{-43}\Delta L(i)/t_{\rm min}(i)$, we find

$$\delta_o \geqslant \left(\frac{\eta_o}{\eta_i}\right)^{1/4+\alpha}, \quad (6)$$

where "$o$" and "$i$" refer to the observed and intrinsic values, respectively. Since the value of $\eta_i$ can be between 0.007 (nuclear reaction) and 0.32 (maximum accretion), we used $\eta_i = 0.05$ (a geometric mean value) in the above equation and found $\delta_o \geqslant 1.17$. Using this $\delta_o$ and an observed $\tau_{\rm var}$ of 142 minutes, we found $R_s < 2.28 \times 10^{14}$ cm.

Considering that the variable emission seen in OJ 287 is due to synchrotron processes, and requiring $\tau_{\rm var}$ to be shorter than the synchrotron lifetime of the relativistic electrons in the observer frame (Hagen-Thorn et al. 2008), the magnetic field ($B$) can be estimated as

$$t_{\rm syn} \propto 4.75 \times 10^2\left(\frac{1+z}{\delta\nu_{\rm GHz}B^3}\right)^{1/2} \text{days}. \quad (7)$$

Using the observed $\tau_{\rm var}$ and $\delta_o$, we find $B \leqslant 3.8$ G. However, using $\delta = 10$ (Baliyan et al. 1996; Marscher & Jorstad 2011; Neronov & Vovk 2011), we find $R_s < 19.5 \times 10^{14}$ cm and $B \sim 1.8$ G. A Doppler factor of 17 has been reported by Aller et al. (2014) based on fits to monitoring observations of OJ 287 in the radio band. Using $\delta = 17$, we obtain $B \sim 1.5$ G, which is close to the value of 0.93 G found in OJ 287 by Baliyan et al. (1996).

Analysis of the long-term variation of PA based on our limited polarimetric observations gives a rotation rate of $5.^{\circ}8$ day$^{-1}$, similar to the value of $4.^{\circ}92$ day$^{-1}$ found by Efimov et al. (2002). This is also in general agreement with the recent results obtained from dedicated optical polarimetric monitoring of blazars, which indicates that the rotation of the plane of optical polarization is a characteristics property of blazars (Blinov et al. 2016). The same set of polarimetric observations also find differences in the polarization properties of different subclasses of blazars (Angelakis et al. 2016). In our polarimetric observations, shown in Figure 6, for most of the epochs we find $P$ to decrease with wavelength. This is similar to that noted by Takalo et al. (1994); however, it is inconsistent with that observed by Tommasi et al. (2001). The observed WDP can be explained in terms of a two-component model identified with the jet that gives rise to the constant polarized component and the shock that gives rise to the more polarized component

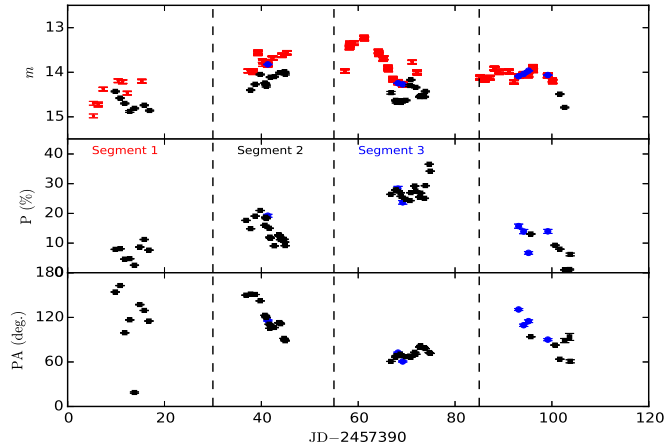


**Figure 7.** Top: long-term variation of $R$-band magnitude ($m_R$) as obtained by us (red) and $V$-band magnitude ($m_V$) as obtained by Steward observatory (black). The $m_R$ corresponding to our polarization measurement is shown in blue. Middle: polarization degree from Steward (black) and obtained by us (blue). Bottom: polarization position from Steward (black) and obtained by us (blue). The data are divided into different segments for detailed analysis. A clear anticorrelation between brightness and polarization can be seen in segment 2.

(Valtaoja et al. 1991). The presence of this stable polarized component is also evident in the position of the average $Q$ and $U$ values that deviate from zero in the $Q$ versus $U$ plane, as seen in Figure 5.

If the accretion disk/host galaxy contributes significantly to the optical emission (in addition to the synchrotron jet emission) of OJ 287, one would have expected higher polarization at longer wavelengths (Malkan & Sargent 1982; Smith et al. 1986). This is not observed in any of our data except that obtained on 2016 February 12, during which epoch the source was in an intermediate brightness state. Also, in the broadband spectral energy distribution of OJ 287, emission from the accretion disk is not prominent (Massaro et al. 2003). Moreover, OJ 287 is a highly core-dominated object,[6] and thus the contribution of the accretion disk to the optical emission of OJ 287 is insignificant. Alternatively, in the binary black hole model of OJ 287, thermal flares are expected when the secondary black hole crosses the accretion disk of the primary black hole. Observations do indicate that such outbursts are not accompanied by increased optical polarization. However, secondary outbursts after the major one do show a correlated behavior in polarization as well, which could be due to the jet of the secondary black hole getting activated. Our polarization observations reported here are during 2016 February–April, much later than the thermal outburst of 2015 December (Valtonen et al. 2016). This, along with other observational evidences outlined above, indicates that the polarization emission during our observations of OJ 287 is mainly due to synchrotron processes happening in the jet of the source.

The LTPV observations show a clear anticorrelation between $P$ and optical brightness, as well as between PA and $P$. These results agree with the polarization monitoring of OJ 287 by Sillanpaa et al. (1991). However, D'arcangelo et al. (2009) noticed a positive correlation between polarization and brightness that is contrary to what we have found. To check for the robustness of our results, we looked for the availability of photometric and polarimetric data during the period of our

[6] The ratio of core to extended emission is >995 (Antonucci & Ulvestad 1985).

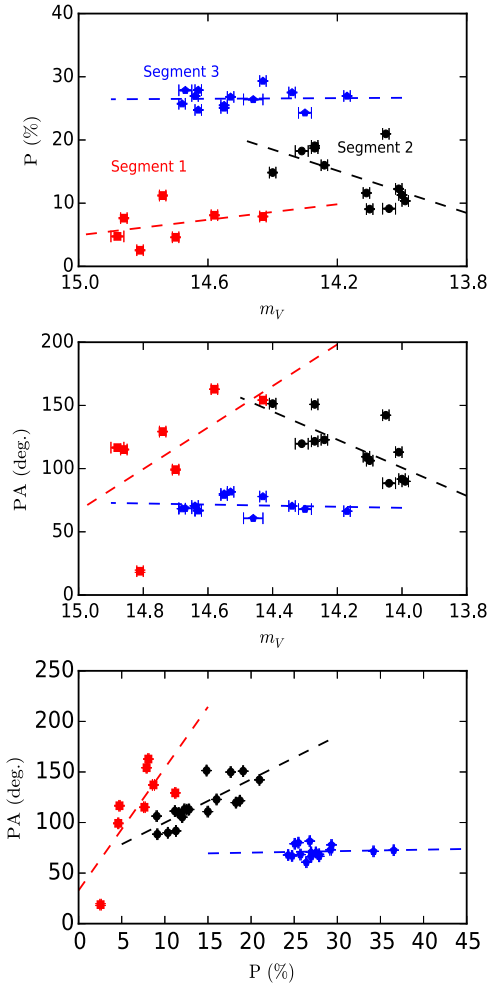


**Figure 8.** Polarization degree vs. $V$-band magnitude (top), PA vs. $V$-band magnitude (middle), and PA vs. polarization degree (bottom) for three different segments as presented in Figure 7. The dotted lines represent the linear fit to the data of each segment.

observation. From the *Fermi* monitoring program of Steward Observatory (Smith et al. 2009) supporting the *Fermi* mission all-sky survey, we collected 48 epochs of polarimetric and 34 epochs of $V$-band photometric data in the period from 2016 January 12 to April 15. The data set and our observations are shown in Figure 7. The data set is divided into four segments based on the seasonal gaps (as shown by dotted lines) for detailed correlation analysis between flux and polarization variations.

In Figure 8, we show the observed relation between flux and polarization behavior of the source for the first three segments. The correlation between these quantities in segment 4 is shown in Figure 4, as the Steward observations have only two epochs of data in this segment. From Figures 8 and 4 it is evident that the brightness of the source positively correlates with polarization during segment 1 (2016 January), correlates negatively during segment 2 (2016 February) and segment 4 (2016 April), and does not show any trend during segment 3 (2016 March). The PA positively correlates with $P$ in segments 1 and 2; however, it correlates negatively in segment 4, and there is no correlation in segment 3. The results of the correlation analysis are given in Table 6.

In the shock-in-jet model of blazar variability, a positive correlation between flux and polarization variations is expected

**Table 6**
Correlation Analysis between Flux and Polarization of OJ 287

| Segment (1) | $P$ versus $V$ (2) | PA versus $V$ (3) | PA versus $P$ (4) |
|---|---|---|---|
| Segment 1 | −0.34 (0.45) | −0.56 (0.19) | 0.74 (0.0327) |
| Segment 2 | 0.55 (0.05) | 0.70 (0.01) | 0.78 (0.0001) |
| Segment 3 | −0.02 (0.92) | 0.10 (0.72) | 0.08 (0.7566) |

**Note.** Columns: (1) segment number; (2) Pearson correlation coefficient of $P$ vs. $V$-band magnitude; (3) PA vs. $V$; (4) $P$ vs. PA. The $p$ value of no correlation is written within parentheses.

(Marscher & Gear 1985), which could be due to the magnetic field getting aligned because of the shock. Alternatively, if the flux variability is due to the emergence of a new blob of plasma (identified as a VLBI scale knot) that has either a chaotic magnetic field or a magnetic field that is misaligned with the large-scale field, an anticorrelation between flux and polarization variations can be expected (Hagen-Thorn et al. 2002; Homan et al. 2002). The observed correlation and anticorrelation between total flux and polarized flux can also be explained by changes in the trajectories of the shocks propagating down the relativistic jets as postulated in the "swinging jets" model of Gopal-Krishna & Wiita (1992). From the observations of OJ 287 reported here we find varied behavior between flux and polarization variations, which could happen because of the presence of more than one emission region in the jet of OJ 287 (Marscher et al. 2008) or due to the interaction between the jet and accretion disk (Valtonen et al. 2008, 2016). Near-simultaneous flux and polarization observations of blazars are very limited, and observations on a large sample of blazars are needed, which will give important leads to our understanding on the emission processes in blazars.

## 5. Conclusions

We have carried out photometric (40 nights) and polarimetric (nine epochs) observations of OJ 287 coinciding with its high brightness state during 2015 December–2016 February. The key findings are summarized below:

1. From 21 nights of INOV observations we found the source to show INOV on a few nights. Using $C$-statistics, we found a DC of INOV of 30%, which increases to 45% and 71% when using the $F$-statistics and $\chi^2$-statistics, respectively. On nights when INOV is observed, $\Psi$ is larger than 3%. The observed large amplitude (>3%) and high DC of INOV are similar to those known for blazars.
2. We find the shortest flux variability timescale of $142 \pm 38$ minutes on 2016 April 07. Using this, we put constraints on the size of the emitting region and magnetic field strength as $2.28 \times 10^{14}$ ($19.5 \times 10^{14}$) cm and 3.8 (1.8) G using $\delta = 1.17$ (10), respectively.
3. Considering LTOV, we find that OJ 287 has varied by about 2 mag during the period of our observations. During this period, it showed a maximum and minimum brightness of $13.20 \pm 0.04$ mag and $14.98 \pm 0.04$ mag, respectively. A change of ∼1 mag was noticed in March within 10 days.
4. From polarimetric observations, we find that OJ 287 showed both INPV and LTPV. Considering the polarization variations during 2016 February to April, minimum and maximum $P$ of $6\% \pm 0.3\%$ and $28.3\% \pm 0.8\%$ in $R$-band were observed. During the same period, PA varied between $60\overset{\circ}{.}6 \pm 0\overset{\circ}{.}8$ and $130\overset{\circ}{.}6 \pm 1\overset{\circ}{.}3$, respectively.
5. In the $U$ vs. $Q$ plane, the average $Q$ and $U$ deviate from zero, indicating the presence of two optically thin synchrotron emission components contributing to the polarized emission from the OJ 287 jet.
6. The $P$ in different wavebands are correlated, with the polarization at shorter wavelengths generally larger than at longer wavelengths, thus showing a WDP behavior. This demands that the observed polarization is due to synchrotron processes happening in the jet of the source.
7. During most of the observing period, an anticorrelation is observed between flux and polarization variations. A wide variety of correlations are also noticed between PA and $P$, as well as between PA and brightness. Such a variety of relations observed between flux and polarization variations might be caused by the presence of more than one emission component in the jet of OJ 287.

We are grateful for the comments and suggestions by the anonymous referee, which helped to improve the manuscript. It is our pleasure to thank A. V. Raveendran and G. Srinivasulu for their valuable suggestions and timely help for the efficient operation of the photopolarimeter. We also thank K. Sagayanathan, A. K. Venkataramana, R. Baskar, S. Surendharnath, A. Muniyandi, A. Ramachandran, M. Muniraj, and the personnel of the technical divisions for their support in carrying out the observations presented in this paper. Data from the Steward Observatory spectropolarimetric monitoring project were used. This program is supported by Fermi Guest Investigator grants NNX08AW56G, NNX09AU10G, NNX12AO93G, and NNX15AU81G.

## References

Agudo, I., Jorstad, S. G., Marscher, A. P., et al. 2011, ApJL, 726, L13
Aharonian, F., Akhperjanian, A. G., Bazer-Bachi, A. R., et al. 2007, ApJL, 664, L71
Aller, M. F., Hughes, P. A., Aller, H. D., Latimer, G. E., & Hovatta, T. 2014, ApJ, 791, 53
Andrew, B. H., Harvey, G. A., & Medd, W. J. 1971, ApL, 9, 151
Andruchow, I., Romero, G. E., & Cellone, S. A. 2005, A&A, 442, 97
Angelakis, E., Hovatta, T., Blinov, D., et al. 2016, MNRAS, 463, 3365
Antonucci, R. R. J., & Ulvestad, J. S. 1985, ApJ, 294, 158
Baliyan, K. S., Joshi, U. C., & Deshpande, M. R. 1996, Ap&SS, 240, 195
Bessell, M. S. 1979, PASP, 91, 589
Bevington, P. R. 1969, Data Reduction and Error Analysis for the Physical Sciences (New York: McGraw-Hill)
Blake, G. M. 1970, ApL, 6, 201
Blinov, D., Pavlidou, V., Papadakis, I., et al. 2016, MNRAS, 462, 1775
Burbidge, G. R., Jones, T. W., & Odell, S. L. 1974, ApJ, 193, 43
Cellone, S. A., Romero, G. E., & Combi, J. A. 2000, AJ, 119, 1534
Ciprini, S., Gasparrini, D., Reyes, L. C., et al. 2009, ATel, 2256, 1
Ciprini, S., Perri, M., Verrecchia, F., & Valtonen, M. 2015, ATel, 8401, 1
D'arcangelo, F. D., Marscher, A. P., Jorstad, S. G., et al. 2009, ApJ, 697, 985
de Diego, J. A. 2010, AJ, 139, 1269
Efimov, Y. S., Shakhovskoy, N. M., Takalo, L. O., & Sillanpää, A. 2002, A&A, 381, 408
Elvis, M., Wilkes, B. J., McDowell, J. C., et al. 1994, ApJS, 95, 1
Escande, L., & Schinzel, F. K. 2011, ATel, 3680, 1
Fabian, A. C., & Rees, M. J. 1979, in X-ray Astronomy, ed. W. A. Baity & L. E. Peterson (Oxford: Pergamon Press), 381
Fiorucci, M., & Tosti, G. 1996, A&AS, 116, 403
Frank, J., King, A. R., & Raine, D. J. 1986, S&T, 71, 579
Gopal-Krishna, & Wiita, P. J. 1992, A&A, 259, 109
Hagen-Thorn, V. A., Larionov, V. M., Jorstad, S. G., et al. 2008, ApJ, 672, 40
Hagen-Thorn, V. A., Larionova, E. G., Jorstad, S. G., Björnsson, C.-I., & Larionov, V. M. 2002, A&A, 385, 55

Homan, D. C., Ojha, R., Wardle, J. F. C., et al. 2002, ApJ, 568, 99
Igumenshchev, I. V., & Abramowicz, M. A. 1999, MNRAS, 303, 309
Jang, M., & Miller, H. R. 1997, AJ, 114, 565
Jones, T. W., Rudnick, L., Aller, H. D., et al. 1985, ApJ, 290, 627
Katz, J. I. 1997, ApJ, 478, 527
Kesteven, M. J. L., Bridle, A. H., & Brandie, G. W. 1976, AJ, 81, 919
Larionov, V. M., Arkharov, A. A., Efimova, N. V., Klimanov, S. A., & Di Paola, A. 2015, ATel, 8374, 1
MacPherson, E., Isler, C. J., Urry, M., et al. 2015, ATel, 8382, 1
Malkan, M. A., & Sargent, W. L. W. 1982, ApJ, 254, 22
Marscher, A. P., & Gear, W. K. 1985, ApJ, 298, 114
Marscher, A. P., & Jorstad, S. G. 2011, ApJ, 729, 26
Marscher, A. P., Jorstad, S. G., D'Arcangelo, F. D., et al. 2008, Natur, 452, 966
Marscher, A. P., & Scott, J. S. 1980, PASP, 92, 127
Massaro, E., Giommi, P., Perri, M., et al. 2003, A&A, 399, 33
Medhi, B. J., Maheswar, G., Brijesh, K., et al. 2007, MNRAS, 378, 881
Muneer, S., Stalin, C. S., Venkataramana, A. K., & Baskar, R. 2016, ATel, 8806, 1
Neha, S., Maheswar, G., Soam, A., Lee, C. W., & Tej, A. 2016, A&A, 588, A45
Neronov, A., & Vovk, I. 2011, MNRAS, 412, 1389
O'Dell, S. L., Puschell, J. J., Stein, W. A., & Warner, J. W. 1978, ApJS, 38, 267
Paliya, V. S., Muneer, S., Venkataramana, C. S. S. A. K., et al. 2016, ATel, 8697, 1
Paliya, V. S., Stalin, C. S., Kumar, B., et al. 2013, MNRAS, 428, 2450
Pursimo, T., Takalo, L. O., Sillanpää, A., et al. 2000, A&AS, 146, 141
Ramaprakash, A. N., Gupta, R., Sen, A. K., & Tandon, S. N. 1998, A&AS, 128, 369
Rautela, B. S., Joshi, G. C., & Pandey, J. C. 2004, BASI, 32, 159
Romero, G. E., Cellone, S. A., & Combi, J. A. 1999, A&AS, 135, 477
Shakhovskoi, N. M., & Efimov, I. S. 1977, IzKry, 56, 39
Shappee, B. J., Stanek, K. Z., Holoien, T. W.-S., et al. 2015, ATel, 8372, 1
Sillanpaa, A., Haarala, S., Valtonen, M. J., Sundelius, B., & Byrd, G. G. 1988, ApJ, 325, 628
Sillanpaa, A., Takalo, L. O., Kikuchi, S., Kidger, M., & de Diego, J. A. 1991, AJ, 101, 2017
Sillanpaa, A., Takalo, L. O., Nilsson, K., Kidger, M., & de Diego, J. A. 1992, A&A, 254, L33
Sillanpaa, A., Takalo, L. O., Pursimo, T., et al. 1996, A&A, 315, L13
Smith, P. S., Balonek, T. J., Heckert, P. A., & Elston, R. 1986, ApJ, 305, 484
Smith, P. S., Montiel, E., Rightley, S., et al. 2009, arXiv:0912.3621
Srinivasulu, G., Raveendran, A. V., Muneer, S., et al. 2015, arXiv:1505.04244
Stalin, C. S., Krishna, Gopal., Sagar, R., & Wiita, P. J. 2004, JApA, 25, 1
Sundelius, B., Wahde, M., Lehto, H. J., & Valtonen, M. J. 1997, ApJ, 484, 180
Takalo, L. O., Sillanpaeae, A., & Nilsson, K. 1994, A&AS, 107, 497
Tommasi, L., Palazzi, E., Pian, E., et al. 2001, A&A, 376, 51
Valtaoja, E., Teräsranta, H., Tornikoski, M., et al. 2000, ApJ, 531, 744
Valtaoja, L., Sillanpaa, A., Valtaoja, E., Shakhovskoi, N. M., & Efimov, I. S. 1991, AJ, 101, 78
Valtonen, M., & Ciprini, S. 2012, MmSAI, 83, 219
Valtonen, M., Zola, S., Gopakumar, A., et al. 2015, ATel, 8378, 1
Valtonen, M. J., Lehto, H. J., Nilsson, K., et al. 2008, Natur, 452, 851
Valtonen, M. J., Mikkola, S., Lehto, H. J., et al. 2011, ApJ, 742, 22
Valtonen, M. J., Zola, S., Ciprini, S., et al. 2016, ApJL, 819, L37
Villata, M., Raiteri, C. M., Sillanpaa, A., & Takalo, L. O. 1998, MNRAS, 293, L13
Villforth, C., Nilsson, K., Østensen, R., et al. 2009, MNRAS, 397, 1893
Wierzcholska, A., & Siejkowski, H. 2015, ATel, 8395, 1
Williamson, K. E., Jorstad, S. G., Marscher, A. P., et al. 2014, ApJ, 789, 135
Xiang, Y., & Dai, B.-Z. 2007, PASJ, 59, 1061
Zhang, L. Z., Fan, J.-H., & Cheng, K.-S. 2002, PASJ, 54, 159
Zola, S., Debski, B., Goyal, A., et al. 2016, ATel, 8667, 1